

ORIGINAL ARTICLE

DNA methylation determines nucleosome occupancy in the 5'-CpG islands of tumor suppressor genes

A Portela¹, J Liz¹, V Nogales¹, F Setién¹, A Villanueva² and M Esteller^{1,3,4}

Promoter CpG island hypermethylation of tumor suppressor genes is an epigenetic hallmark of human cancer commonly associated with nucleosome occupancy and the transcriptional silencing of the neighboring gene. Nucleosomes can determine the underlying DNA methylation status. Herein, we show that the opposite is also true: DNA methylation can determine nucleosome positioning. Using a cancer model and digital nucleosome positioning techniques, we demonstrate that the induction of DNA hypomethylation events by genetic (DNMT1/DNMT3B deficient cells) or drug (a DNA demethylating agent) approaches is associated with the eviction of nucleosomes from previously hypermethylated CpG islands of tumor suppressor genes. Most importantly, the establishment of a stable cell line that restores DNMT1/DNMT3B deficiency shows that nucleosomes reoccupy their positions in *de novo* methylated CpG islands. Finally, we extend these results to the genomic level, combining a DNA methylation microarray and the nucleosome positioning technique. Using this global approach, we observe the dependency of nucleosome occupancy upon the DNA methylation status. Thus, our results suggest that there is a close association between hypermethylated CpG islands and the presence of nucleosomes, such that each of these epigenetic mechanisms can determine the recruitment of the other.

Oncogene (2013) 32, 5421–5428; doi:10.1038/onc.2013.162; published online 20 May 2013

Keywords: DNA methylation; tumor suppressor gene; nucleosome; CpG island; DNA methyltransferase

INTRODUCTION

In general, CpG island methylation is associated with gene silencing.¹ CpG islands are usually unmethylated in normal cells, although some of them (~6%) become methylated in a tissue-specific manner during development or in differentiated tissues.² However, in tumoral cells many tumor suppressor genes are silenced through CpG island methylation.^{1–3} Hypermethylated promoters are also associated with a closed chromatin configuration, characterized by a histone modification pattern featuring deacetylation of histones H3 and H4, methylation of histone H3 lysines 9 and 27 and demethylation of histone H3K4.^{1–4}

It is also important to keep in mind the packaging of the DNA into nucleosomes. Nucleosomes can act as a barrier to transcription, regulating access to the DNA in the nucleus. During transcription elongation, the DNA is unwrapped from the nucleosome, allowing the RNA polymerase II to progress.⁵ In fact, the precise position of nucleosomes around the transcription start sites (TSSs) can be crucial to gene expression regulation.⁶ The loss of a nucleosome directly upstream of the TSS is closely correlated with gene activation, whereas the occlusion of the TSS by a nucleosome is associated with gene repression.^{7–8} The relationship between DNA methylation and nucleosome positioning has been precisely described in the *mutL* homolog 1 (*MLH1*) gene: a methylated CpG island prevents nucleosome depletion from the promoter, thereby reducing the *MLH1* transcription level.⁹ In this regard, DNA methyltransferases

(DNMTs) are preferentially targeted to nucleosome-bound DNA, even for methylated non-CpG island promoters.¹⁰ Thus, nucleosome positioning should help shape the DNA methylation landscape.^{11–12} Other DNA methylation-related enzymes (methyl-CpG binding domain protein 2, MBD2; methyl-CpG binding protein 2, MeCP2) are also known to be enriched when nucleosomal methylated DNA is compared with methylated DNA.¹³ The effect of DNA methylation in the nucleosomal context enhances transcription repression, as CpG methylation induces tighter wrapping of DNA around the histone core and a change in topology.¹⁴

The objective of our study was to shed light on the relationship between nucleosome positioning and DNA methylation, assessing whether it is a unidirectional or a bidirectional phenomenon. Nucleosome positioning can direct DNA methylation patterns,^{11–12} but can DNA methylation also determine nucleosome positioning?

RESULTS

Local relationship between DNA methylation, gene expression and nucleosome positioning

We studied both DNA methylation and nucleosome occupancy in the colorectal cancer cell line HCT-116 and its isogenic cell line with double knockout of the DNA methyltransferases DNMT1 and DNMT3B (DKO).¹⁵ We also studied the DNA hypomethylation

¹Cancer Epigenetics and Biology Program (PEBC), Bellvitge Biomedical Research Institute (IDIBELL), L'Hospitalet, Barcelona, Catalonia, Spain; ²Translational Research Laboratory, Catalan Institute of Oncology, Bellvitge Biomedical Research Institute (IDIBELL), L'Hospitalet, Barcelona, Catalonia, Spain; ³Department of Physiological Sciences II, School of Medicine, University of Barcelona, Barcelona, Catalonia, Spain and ⁴Institució Catalana de Recerca i Estudis Avançats (ICREA), Barcelona, Catalonia, Spain. Correspondence: Dr M Esteller, Cancer Epigenetics and Biology Program (PEBC), Bellvitge Biomedical Research Institute (IDIBELL), L'Hospitalet, 3rd Floor, Hospital Duran i Reynals, Avda Gran Via Km 2.7, Barcelona, Catalonia 08908, Spain.

E-mail: mesteller@idibell.cat

Received 14 December 2012; revised 11 March 2013; accepted 18 March 2013; published online 20 May 2013

events and their association with putative nucleosome eviction in the HCT-116 cell line treated with the demethylating agent 5-aza-2'-deoxycytidine (Aza). We also wondered whether the association between DNA methylation and nucleosome positioning could be established *de novo*. To this end, we generated a new cell line (DKO DNMT1/3B), stably reintroducing DNMT1 and DNMT3B into the DKO cell line (Supplementary Figure S1). Since the original description of the DKO cells, several articles have dealt with the biological features of these cells,^{16–18} but herein, we have also developed doubling time determination, colony formation, MTT (3-[4,5-dimethylthiazol-2-yl]-2,5 diphenyl tetrazolium bromide) and nude mice subcutaneous growth assays for HCT-116, DKO and DKO DNMT1/3B cells (Supplementary Methods). Overall, DKO cells has a slower growth in doubling time, colony formation, MTT and *in vivo* nude mouse tumor-growth assays in comparison with parental HCT-116 cells, while the reintroduction of DNMT1/DNMT3B enhances the growth of DKO cells in the three analyses. (Supplementary Figure S1).

In order to test our hypothesis that DNA methylation can determine nucleosome occupancy, we selected two well-known 5'-hypermethylated CpG islands of the tumor suppressor genes retinoic acid receptor beta (*RARB*)¹⁹ and homeobox D1 (*HOXD1*)¹⁶ and two recently identified, potassium voltage-gated channel subfamily G member 2 (*KCNG2*) and nephosis 2 idiopathic steroid-resistant (*NPHS2*).²⁰ The corresponding 5'-ends of these genes are annotated as CpG islands by the University of California Santa Cruz, UCSC and The National Center for Biotechnology Information, NCBI genome browsers, except for *RARB* that it is only formally recognized as a classical and canonical CpG island by the NCBI data set, although it has been widely studied as such.¹ For the four genes, we validated their DNA methylation status, levels of expression and nucleosome positioning structure in an average 850 bp area centered on their TSS. Bisulfite sequencing (Figure 1a and Supplementary Figure S2) was used for the DNA methylation analyses, while expression was determined by quantitative real-time PCR (Figure 1b) and semi-quantitative reverse transcriptionPCR (Supplementary Figure S3). The studies were performed in the following cell lines: HCT-116, HCT-116 Aza, DKO and DKO DNMT1/3B. As a control, the same characteristics were studied in the glyceraldehyde-3-phosphate dehydrogenase gene (*GAPDH*) (Supplementary Figure S2) and the tumor suppressor *p53* (Supplementary Figure S4), which are unmethylated and exhibit a similar expression pattern in all cell lines used here. DNA methylation status was checked in three overlapping regions: one located upstream of the TSS, another containing the TSS and the third downstream of the TSS (Figure 1a, Supplementary Figure S2 and the primers are described in Supplementary Table S1). The methylation patterns for each gene were consistent in each case for the three regions studied. HCT-116 cells presented *HOXD1*, *RARB*, *KCNG2* and *NPHS2* hypermethylated CpG island promoters (Figure 1a and Supplementary Figure S2), and accordingly, no transcripts were expressed (Figure 1b and Supplementary Figure S3). On the other hand, *GAPDH* and *p53* (Supplementary Figure S4) promoters were unmethylated and the genes were expressed. In the DKO cell line, the four promoters were unmethylated (Figure 1a and Supplementary Figure S2) and so expressed the four transcripts (Figure 1b and Supplementary Figure S3). When treating the HCT-116 cell line with the DNA demethylating agent 5-aza-2'-deoxycytidine for 72 h the level of CpG methylation decreased (Figure 1a and Supplementary Figure S2) with a concordant reactivation of transcription in the *HOXD1*, *RARB*, *KCNG2* and *NPHS2* genes (Figure 1b and Supplementary Figure S3). The stable reintroduction of DNMT1 and DNMT3B into the DKO cell line partially restored the methylation pattern of *HOXD1*, *RARB*, *KCNG2* and *NPHS2* genes (Figure 1a), while the *GAPDH* (Supplementary Figure S2) and *p53* (Supplementary Figure S4) genes remained unmethylated. As expected, the levels of expression of *HOXD1*, *RARB*, *KCNG2* and

NPHS2 genes were lower in the DKO DNMT1/3B cell line than in the DKO cell line (Figure 1b and Supplementary Figure S3).

To assess the chromatin structure in the selected promoters, we sought to obtain a general overview using the *MspI* accessibility assay coupled to a real-time PCR, thereby to quantify the data. The *MspI* accessibility assay is based on the chromatin structure: the tighter the chromatin is packed, the less accessible it is to the restriction enzyme. Thus, in an extreme case, the chromatin would be so tightly packaged that the restriction sites would not be accessible, thereby preventing the enzyme from digesting the DNA, even when increasing units of restriction enzyme were used. Conversely, the less compact the chromatin structure is, the greater the digestion achieved when using increasing units of the selected restriction enzyme (*MspI*). Therefore, a PCR performed on a particular region will give an amount of product indirectly proportional to the chromatin accessibility. To achieve greater accuracy and reproducibility, we performed a semi-quantitative real-time PCR to measure the amount of product obtained in each case. HCT-116, HCT-116 treated with Aza, DKO and DKO DNMT1/3B nuclei were extracted and incubated with increasing concentrations of *MspI* restriction enzyme (0, 100 and 400 U/ml). Moreover a positive control of non-digested DNA and a negative control of 100% digested DNA were also analyzed. For each gene, three overlapping regions were studied: one located upstream of the TSS, another containing the TSS and the third downstream of the TSS. The results obtained were similar for all the studied regions in each gene. The DKO cell line presented lower levels of amplification as the number of restriction enzyme units rose in all genes tested (*GAPDH*, *HOXD1*, *RARB*, *KCNG2* and *NPHS2*), thereby revealing a more open chromatin structure (Figure 2a and Supplementary Figure S5). DKO cells are not 100% fully accessible to the enzymes because this cell line has not lost completely DNA methylation.¹⁵ On the other hand, the HCT-116 cell line presented a lower degree of amplification following *MspI* digestion, and thus an open chromatin structure only in the *GAPDH* (Figure 2a and Supplementary Figure S5 data for *MspI* 400 U/ml; Supplementary Figure S6 data for *MspI* 100 U/ml) and *p53* (Supplementary Figure S4) genes. Thus, these regions seem to be inaccessible to *MspI* in HCT-116 cell line and are considered to have denser nucleosome occupancy. When treating the HCT-116 cell line with 5-aza-2'-deoxycytidine, the chromatin structure resembled that observed in the DKO cell line, with higher DNA accessibility than untreated HCT-116 cells (Figure 2a and Supplementary Figures S5 and S6). In this regard, drug depletion of DNA methylation (5-aza-2'-deoxycytidine treatment) resembled the genetic depletion of DNMTs (DKO cells) for the DNA methylation pattern, the expression levels and the chromatin accessibility assays. When DNMT1 and DNMT3B were stably reintroduced to the DKO cell line (DKO DNMT1/3B), denser nucleosome occupancy was observed, correlating with the partial recovery of DNA methylation in the promoters and a decrease in gene expression (*HOXD1*, *RARB*, *KCNG2* and *NPHS2*). The results obtained were consistent in the three studied regions of each gene.

To avoid the false positive results in the *MspI* assay in case one primer is positioned in the linker of a nucleosome occupied region, we also designed an additional set of primers for these experiments and the same data were obtained (Supplementary Figure S7). In addition, although a NaCl (0.4 M) wash was used in our assays to remove most non-histone-bound proteins from chromatin,²¹ DNA accessibility could not fully reflect nucleosomes as the binding of other proteins to DNA may also affect the sensitivity to the restriction enzymes. Thus, we analyzed the presence of a core histone protein to provide a more direct analysis of nucleosomes. Using chromatin immunoprecipitation analyses for the core histone H3, we found that the hypermethylated promoter CpG islands of *HOXD1*, *RARB*, *CDH11* and *SCGB3A1* in HCT-116 cells are enriched in histone H3 (Supplementary Figure S8). In contrast, the unmethylated

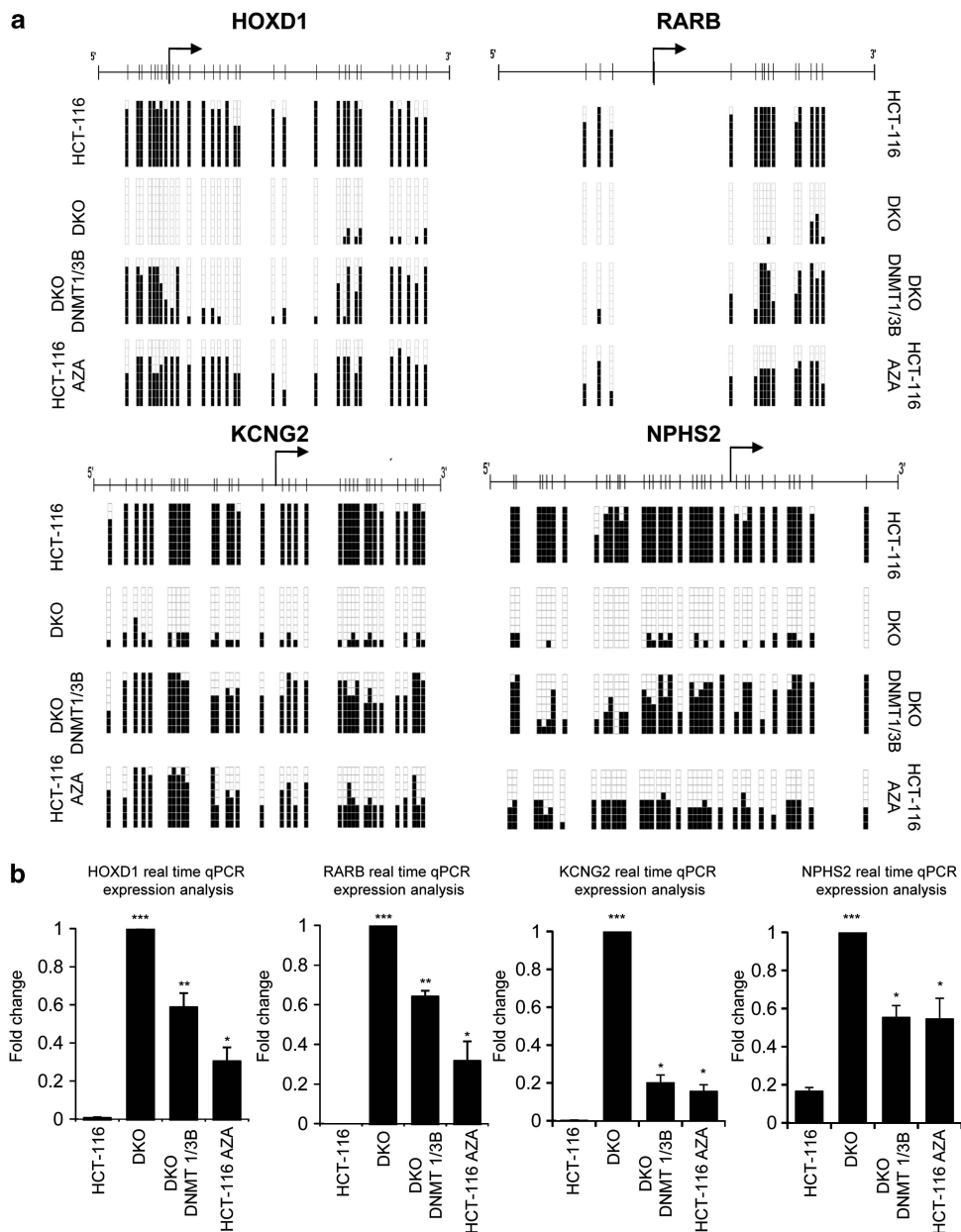


Figure 1. 5'-CpG island DNA methylation is associated with transcriptional silencing. (a) DNA methylation status of the region containing the TSS is shown (regions upstream and downstream of the TSS are shown in Supplementary Figure S2). In each case, eight bisulfite-modified clones were sequenced. Black and white squares correspond to methylated and unmethylated CpG, respectively. (b) Expression of *HOXD1*, *RARB*, *KCNG2* and *NPHS2* is shown for all the cell lines and cases studied. Statistical significance in real-time experiments has been assessed with an analysis of variance (ANOVA) test (* $P < 0.05$, ** $P < 0.01$, *** $P < 0.001$).

promoter CpG islands of the four genes in DKO cells show a depletion of core histone H3 (Supplementary Figure S8).

To measure nucleosome occupancy more accurately, we adapted the methyltransferase-based single-promoter analysis assay protocol,²¹ to make it suitable for studying methylated DNA sequences (Figure 2b). For our purpose we used *MspI*, *HaeIII* and *AluI* methyltransferases, which modify the cytosine residue (C⁵) of the CCGG (external C), GGCC (internal C) and AGCT sites, respectively. The use of the three methyltransferases allowed us to increase the resolution of the *in vitro* methylation maps obtained. HCT-116, DKO, HCT-116 treated with Aza and DKO DNMT1/3B extracted nuclei were *in vitro* methylated using the three methylases in a sequential incubation. Bisulfite sequencing was then performed in the regions of interest

(Figure 2c and Supplementary Figures S9). Again, for each gene, three overlapping regions were studied: one upstream of TSS, another containing the TSS and the third downstream of the TSS. The regions queried in the methyltransferase-based single-promoter analysis assay experiments were all over 147 bp in length to ensure nucleosome occupancy with an average size of 243 bp (PCR amplicon sizes are detailed in Supplementary Table S1). The results were similar for all the regions studied in each gene and completely complementary to those obtained with the *MspI* accessibility assay, although of higher resolution (Figure 2c and Supplementary Figures S9). It is interesting to note that greater differences in nucleosome occupancy were observed in the region containing the TSS. An open chromatin state was confirmed for *HOXD1*, *RARB*, *KCNG2* and *NPHS2* genes in

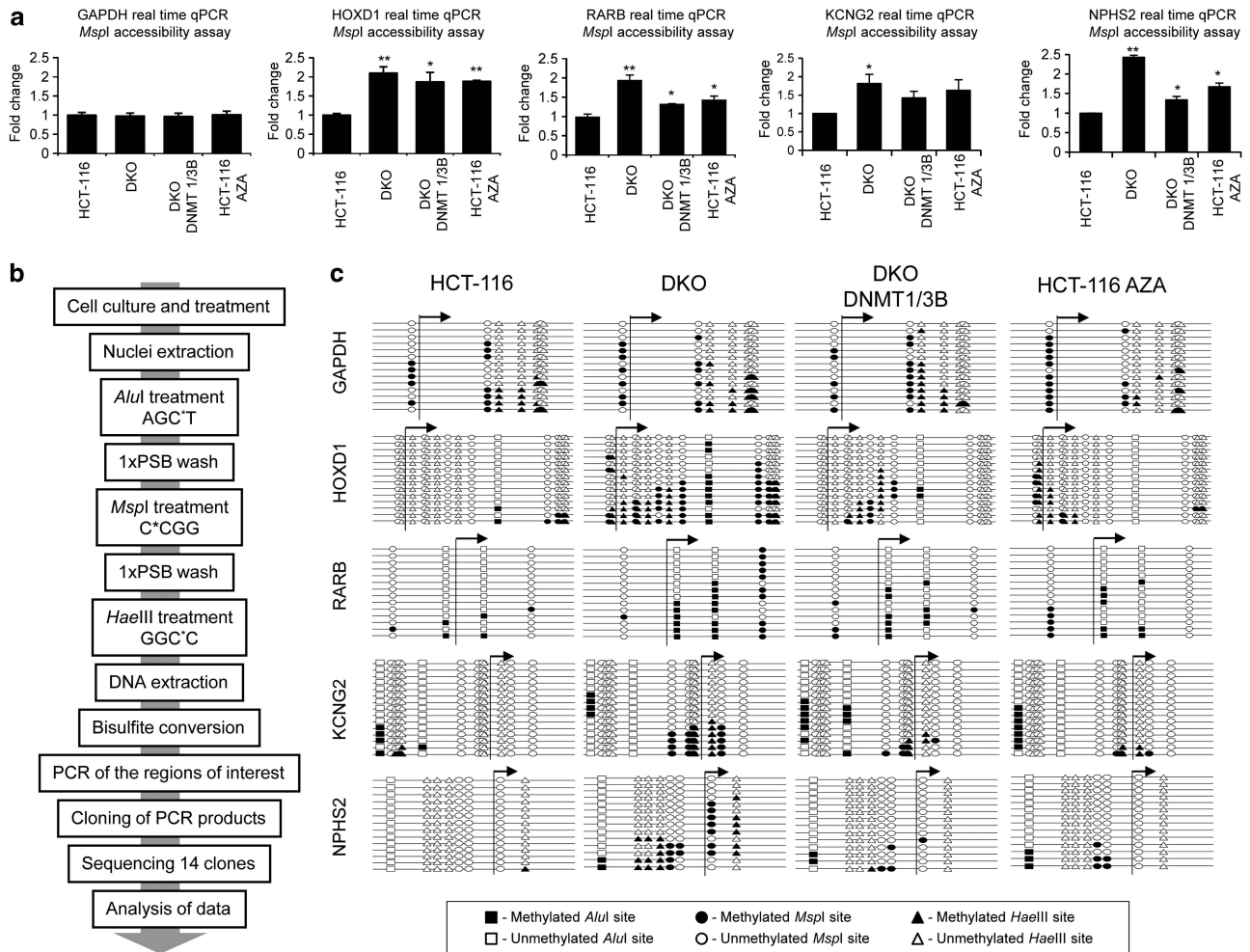


Figure 2. DNA methylation determines nucleosome positioning. **(a)** *MspI* accessibility assay. Results are depicted as the *n*-fold difference between undigested DNA and 400 U/ml digested DNA. Only the results from the region containing the TSS are presented (regions upstream and downstream of the TSS are shown in Supplementary Figure S5). The results of the *MspI* accessibility assay are correlated with nucleosome occupancy. The results represent the ratio undigested/digested for each sample normalized to undigested/digested for HCT116. **(b)** Adaptation of the methyltransferase-based single-promoter analysis assay (M-SPA) protocol for use in studying methylated sequences. **(c)** Adapted M-SPA protocol for studying the same regions studied in **(a)** at higher resolution. Circles, triangles and squares, respectively, represent methylation sites of *MspI* (C*CGG), *HaeIII* (GGC*C) and *AluI* (AGC*T). Black and white figures represent methylated and unmethylated sites, respectively. Accessible regions, in which nucleosomes are not present, become methylated, whereas inaccessible regions do not. Only the results from the region containing the TSS are presented (regions upstream and downstream of the TSS are shown in Supplementary Figure S9). Statistical significance in real-time experiments has been assessed with an ANOVA test (* $P < 0.05$, ** $P < 0.01$, *** $P < 0.001$).

DKO cells, whereas a closed chromatin state was observed in HCT-116 cells. Treatment of HCT-116 cells with Aza loosened nucleosome positioning, while reintroduction of DNMT1 and DNMT3B activity in DKO cells resulted in nucleosome repositioning.

We also performed a time course study for DNA methylation and nucleosome occupancy in HCT-116 cells upon the use of the DNA demethylating agent using sixteen different time points (Supplementary Figures S10). We have determined the DNA methylation content and *MspI* accessibility of the three studied regions of the *HOXD1* and *RARB* promoter CpG islands for 192 h at 12-h intervals: six time points with continuous Aza treatment and ten time points after Aza withdrawal (a total of 16 time points). We have observed that the highest point of DNA accessibility is observed 12 h later than the highest point of DNA hypomethylation (Supplementary Figure S10), suggesting that nucleosome eviction might occur afterwards the loss of DNA methylation. In addition, the withdrawal of the demethylating drug from the media caused a progressive reduction of gene expression (Supplementary Figure S11).

DNA methylation-nucleosome occupancy relationship is a genome-wide phenomenon

Having demonstrated the relationship between DNA methylation and nucleosome occupancy for particular genes, we wondered about the extent of these mechanisms at a more global genomic level. To address this, genomic and mononucleosomal DNAs from HCT-116 and DKO cell lines were obtained and hybridized to the Golden-Gate DNA methylation BeadArray (Illumina Inc., San Diego, CA, USA), which contains 1505 CpG sites located between -1500 bp and $+500$ bp around the TSSs of 808 cancer-related genes^{22–25} (Figure 3a). The data were analyzed as follows (Figure 3b). Sequences were considered to be hypermethylated when the difference in CpG β -values between the HCT-116 and DKO cell lines was $\geq 70\%$. The first comparison was made of the genomic DNA from the HCT-116 and DKO cell lines. This allowed us to select hypermethylated regions in the HCT-116 cell line (272 CpG sites corresponding to 190 genes). Mononucleosomal HCT-116 and genomic DKO data were then compared. This second comparison enabled the selection of hypermethylated HCT-116

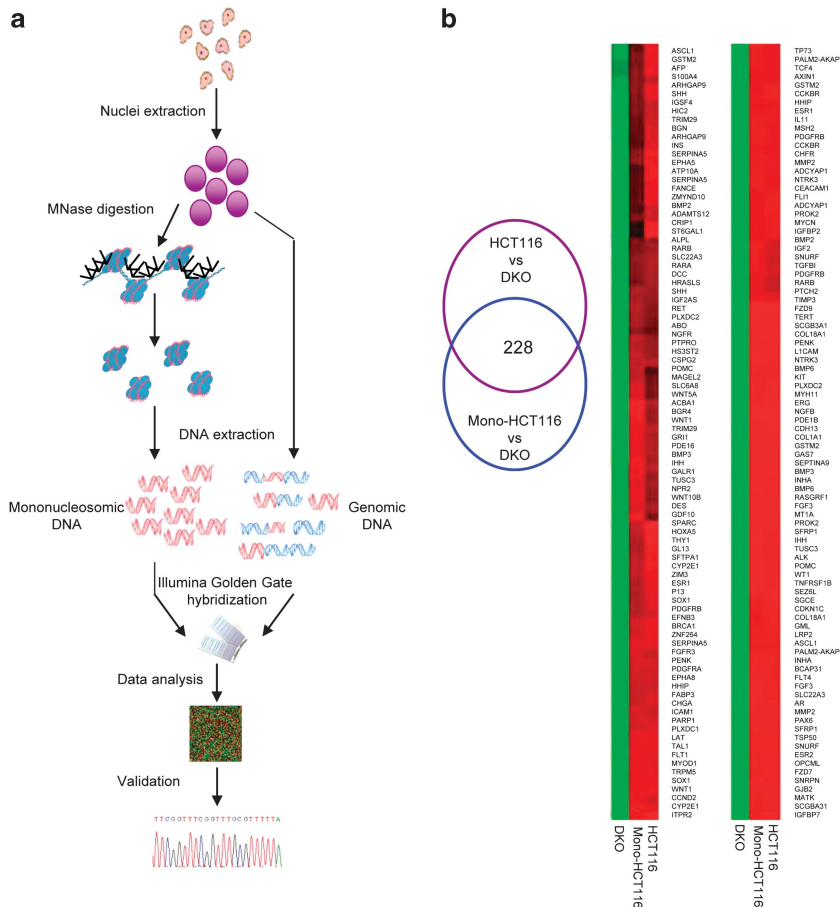


Figure 3. Genome-wide approach for DNA methylation and nucleosome positioning. **(a)** Detailed flowchart of the protocol followed to obtain genome-wide data. **(b)** Analysis of genome-wide data. The Venn diagram shows the analysis done to select the DNA-methylated regions that are protected by nucleosomes. Images below are of two significant regions of the DNA methylation microarray. Green rectangles, unmethylated DNA sequences; Red rectangles, methylated DNA sequences.

regions that had escaped micrococcal nuclease digestion due to their location around a nucleosome (252 CpG sites corresponding to 181 genes). The DKO mononucleosomal data were used as a negative control, confirming that the unmethylated regions are more easily digested by the micrococcal nuclease, as most of them are not protected by a nucleosome. Finally, the joint consideration of both comparisons enabled us to select the genomic hypermethylated regions that had been protected from MNase digestion due to their location around a nucleosome. The overlapping region contained 228 probes corresponding to 162 genes (Supplementary Table S2). Thus, around 84% (83.82% in the context of probes and 84.21% in that of genes) of the hypermethylated regions selected in the genomic DNA from the HCT-116 cell line were conserved in the mononucleosomal HCT-116 DNA, meaning that 84% of the hypermethylated regions are occupied by nucleosomes. The genome-wide results clearly highlight the strong relationship between DNA methylation and nucleosome positioning, implying that this relationship is standard in methylated sequences, rather than being a rare phenomenon.

To start the validation of the array results, we first confirmed that the initially studied candidate gene *RARB* was also identified in the genome-wide approach as having a hypermethylated promoter CpG island occupied by nucleosomes (Supplementary Table S2). CpG sites for the other three candidate genes (*HOXD1*, *KCNG2* and *NPHS2*) were not printed in the used DNA methylation microarray platform and, thus, could not be characterized. To further validate the array data, two candidate genes obtained by the

forementioned epigenomic approach, were selected for further detailed study: cadherin-11 (*CDH11*), a tumor suppressor gene within our area of expertise²⁶ and secretoglobin-3A1 (*SCGB3A1*), a randomly selected candidate gene to avoid any kind of functional bias. Both genes were analyzed to examine their DNA methylation (Figure 4a and Supplementary Figure S12), gene expression (Figure 4b) and nucleosome occupancy level (Figures 4c and d and Supplementary Figure S13). In these cases, the DNA methylation profile was studied in three regions (upstream of the TSS, containing the TSS and downstream of the TSS) for both genes. However, the *MspI* accessibility assay was only performed in two regions (upstream of the TSS and containing the TSS) on the *CDH11* gene, as the region downstream of the TSS did not contain an *MspI* restriction site. Again, the results obtained for the different regions of each gene were consistent in each cell line studied. *CDH11* and *SCGB3A1* were methylated in the HCT-116 cell line and unmethylated in the DKO. Treatment of HCT-116 cells with the demethylating agent Aza, partially reduced DNA methylation in all the studied regions. Reintroduction of DNMT1 and DNMT3B activity in the DKO cell line partially remethylated the regions studied (Figure 4a and Supplementary Figure S12). DNA methylation (HCT-116 and DKO DNMT1/3B) was always associated with the suppression or reduction of expression, while unmethylated promoters (DKO) or reduction of the methylation (HCT-116 Aza) was associated with an increase in transcription (Figure 4b).

CDH11 and *SCGB3A1* genes were also evaluated at the nucleosome occupancy level through an *MspI* accessibility assay (Figure 4c and Supplementary Figure S13) and adapted

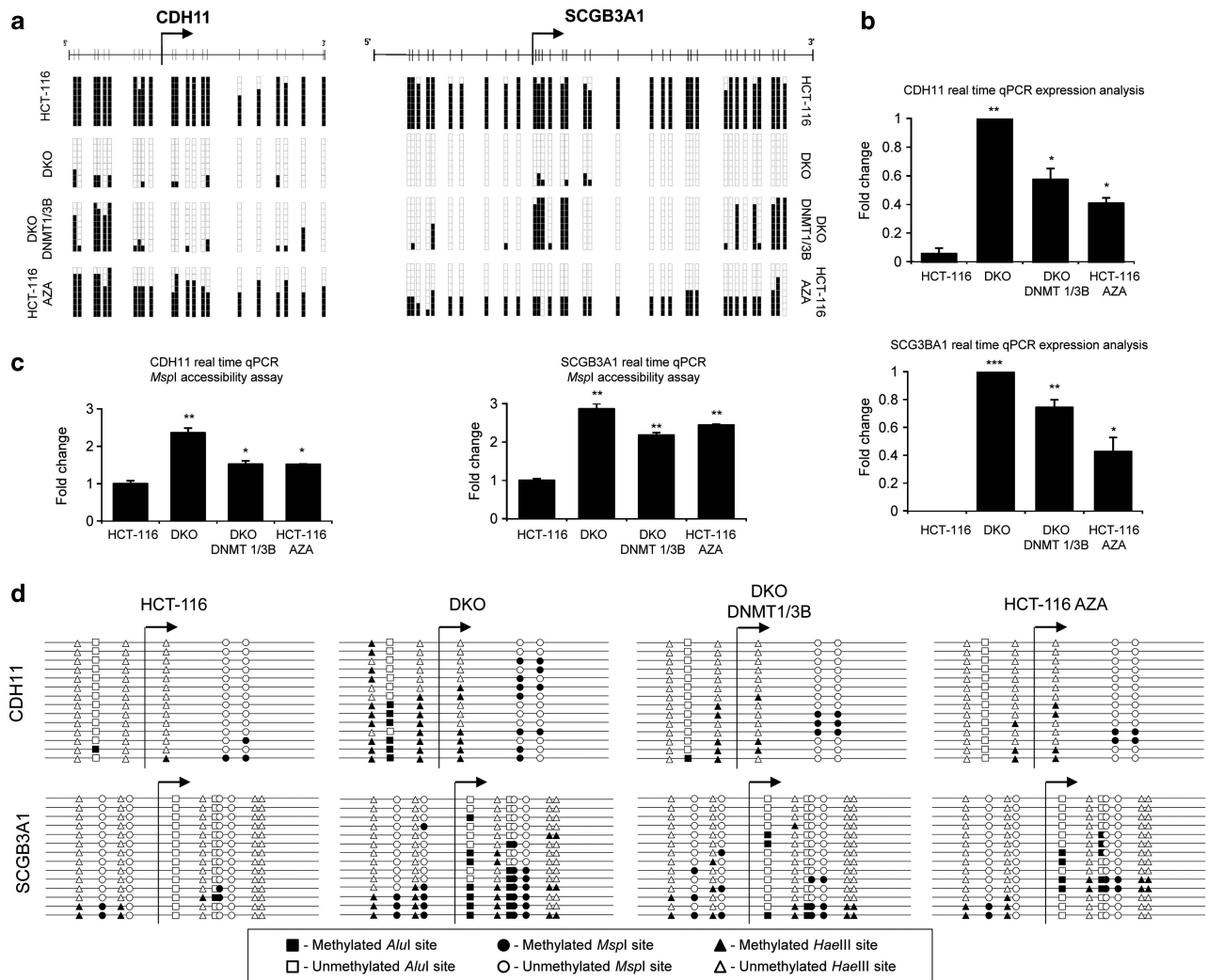


Figure 4. DNA methylation, expression and nucleosome positioning of the candidate genes obtained from the array. **(a)** DNA methylation status of the region containing the TSS is shown in the genes selected to validate the arrays: *CDH11* and *SCGB3A1* (regions upstream and downstream of the TSS are shown in Supplementary Figure S12). In each case, eight bisulfite-modified clones were sequenced. Black and white squares correspond to methylated and unmethylated CpG, respectively. **(b)** *CDH11* and *SCGB3A1* expression determined by quantitative PCR. **(c)** *MspI* accessibility assay. The results are depicted as the n-fold difference between undigested DNA and 400 U/ml digested DNA. Only the results from the region containing the TSS are presented (regions upstream and downstream of the TSS are shown in Supplementary Figure S13). **(d)** Adapted M-SPA protocol for studying the same regions as in **(a)** at higher resolution. Circles, triangles and squares, respectively, represent methylation sites of *MspI* (C*CGG), *HaeIII* (GGC*C) and *AluI* (AGC*T). Black and white figures represent methylated and unmethylated sites, respectively. Accessible regions, in which nucleosomes are not positioned, become methylated, while inaccessible regions remain unmethylated. Only the results from the region containing the TSS are presented (regions upstream and downstream of the TSS are shown in Supplementary Figure S13). Statistical significance in real-time experiments has been assessed with an ANOVA test (* $P < 0.05$, ** $P < 0.01$, *** $P < 0.001$).

methyltransferase-based single-promoter analysis assay (Figure 4d and Supplementary Figure S13) techniques. Again DNA methylation and transcription repression was associated with dense nucleosome occupancy in the HCT-116 cell line, while unmethylated DNA was associated with a high level of expression and low nucleosome occupancy in the DKO cell line (Figure 4 and Supplementary Figures S12 and S13). Reduction of DNA methylation in the HCT-116 cell line upon Aza treatment or reintroduction of the DNMT1 and DNMT3B activity in the DKO cell lines created intermediate outcomes, with around 50% DNA methylation (Figure 4a and Supplementary Figure S12), intermediate expression (Figure 4b) and intermediate nucleosome occupancy (Figures 4c and d and Supplementary Figure S13). To avoid the false positive results in the *MspI* assay in case one primer is positioned in the linker of a nucleosome occupied region, we also designed an additional set of primers for these experiments and the same data were obtained (Supplementary Figure S14).

Thus, both the candidate gene approach and the genomics assay support the conclusion that DNA methylation at the 5'-CpG island of tumor suppressor genes contributes to determine nucleosome occupancy at these regions and that DNA hypomethylation events remove nucleosomes from these CpG-rich sequences surrounding the respective TSSs.

DISCUSSION

The wrapping of DNA around nucleosomes⁶ and DNA methylation¹ are two well-known mechanisms involved in gene expression regulation. However, as has recently been reported, the occurrence of these phenomena seems to be closely associated rather than independent.^{11–12} On one hand, despite the obstacle of reaching the DNA that a nucleosome might present to an enzyme, the DNMT1 and DNMT3B enzymes are both able to methylate CpG sites on nucleosomes assembled *in vitro*.²⁷

Nucleosomal DNA is more methylated than flanking DNA, suggesting that DNMTs might be easily recruited to nucleosome-bound DNA, enhancing DNA methylation in nucleosomal DNA.¹¹ In this regard, it is interesting to see the remethylation patterns obtained when DNMT1 and DNMT3B are stably reintroduced in the DKO cell line. The presence of nucleosomes enhances the recruitment of DNMTs, making methylation of the DNA that wraps the nucleosome easier.^{6–28} It has been shown that DNMT3A and DNMT3B are strongly anchored to nucleosomes containing methylated DNA.²⁹ In fact, this anchoring serves as a positive feedback mechanism, allowing the faithful propagation of the DNA methylation pattern through somatic cell divisions, and preventing DNMT3A and DNMT3B degradation.³⁰ Thus, nucleosome positioning helps shape the DNA methylation landscape.¹¹ However, in the remethylated regions studied in the DKO DNMT1/3B, no nucleosomes were positioned in the original DKO cell line. Thus it is improbable that nucleosomes could guide the remethylation process in the DKO DNMT1/3B cell line. Moreover, the lengths of more highly methylated regions in the DKO DNMT1/3B cell line are not associated with nucleosomal DNA length (~147 bp). It is therefore conceivable that this also occurs the other way around: reintroduction of DNMT1 and DNMT3B in DKO cell line methylates DNA, nucleosomes become positioned and thus transcription is repressed. Methylation and nucleosome occupancy would act cooperatively to repress transcription.^{14–31}

On the other hand, other reports have proposed that DNMT1 is only loosely associated with chromatin, mostly at linker or nucleosome-free regions, while DNMT3A and DNMT3B tend to be associated with nucleosomes containing already methylated DNA.²⁹ Indeed, in mammals, an I662N substitution in DNMT3B is responsible for the higher affinity of this enzyme for nucleosomal DNA.²⁸ Moreover, DNA methylation also seems to influence the structural properties of DNA, reducing the affinity of DNA for the histone octamer.³² However, the detected changes in nucleosome formation and translational positioning according to the CpG methylation status of the studied genes were subtle.³³ Furthermore, the decreased affinity of the octamer by methylated DNA²⁹ might suggest that our observed nucleosome depletion upon DNA hypomethylation events, might involve additional structural constraints other than simple histone/DNA interactions. The complexity of the process is shown by the finding that, although in the majority of the genome, nucleosomal DNA is preferentially methylated,¹¹ specific sequences such as CTCF (CCCTC-binding factor) sites might not adhere to this trend.³⁴

Our data suggest that DNA methylation and nucleosome positioning shape each other in a complementary, bidirectional manner: in our model, DNA methylation determines nucleosome positioning, but in other contexts nucleosome occupancy determines DNA methylation patterns. In our study, DNA hypermethylated 5'-CpG islands (HCT-116) were always associated with low or null levels of gene expression, while unmethylated promoters (DKO) were correlated with higher levels of gene expression. In addition, transcriptional repression was also correlated with closed chromatin domains with dense nucleosome occupancy, while actively transcribed genes had lower nucleosome occupancy levels. 5-aza-2'-deoxycytidine treatment and DKO cells had reduced DNA methylation levels, increased gene transcription and decreased nucleosome occupancy, relative to the untreated/wild-type HCT-116 cell line. Reintroduction of DNMT1 and DNMT3B activity in the DKO cells caused an increase of DNA methylation, repression of gene transcription and an increase in nucleosome occupancy. These results suggest a close correlation between DNA methylation, transcriptional repression and high nucleosome occupancy. This relationship is not only local but also genome-wide. In addition, if nucleosome positioning affects the DNA methylation landscape,^{11–12} our evidence suggests that the reciprocal process might also occur.

MATERIALS AND METHODS

Human cancer cell lines

HCT-116 colon cancer cells and double DNMT1 –/– and DNMT3B –/– (DKO) cells were grown as previously described.¹⁵ HCT-116 cells were treated with 5-aza-2'-deoxycytidine (1 μM) for 72 h. The DKO DNMT1/3B cell line was obtained by stably reintroducing the DNMT1 (cloned in a pCDNA3 vector with Zeocin resistance) and DNMT3B (cloned in a pRES vector with Puromycin resistance) genes. The DKO DNMT1/3B cells were cultured in 1/400 Zeocin and 4.7 Puromycin concentrations.

DNA methylation analysis

DNA methylation was determined by PCR analysis after bisulfite modification. Bisulfite genomic sequencing was carried out as previously described.¹⁶ A minimum of eight colonies of each sequence and sample were automatically sequenced to determine the pattern of methylation. Bisulfite genomic-sequencing primers are shown in Supplementary Table S1.

Quantitative reverse-transcription PCR expression analysis

RNA was isolated with TRIzol (Invitrogen, Grand Island, NY, USA) according to the manufacturer's instructions. Total RNA was then treated with DNase I (Ambion, Grand Island, NY, USA), and 1 μg was retrotranscribed with Superscript II reverse transcriptase (Life Technologies, Grand Island, NY, USA). Real-time PCRs were performed in an Applied Biosystems 7900HT Fast Real-Time PCR System, using 40 ng of complementary DNA for each amplification. Expression values were normalized with respect to *GAPDH* expression. Reverse-transcription PCR primers were designed in different exons to prevent DNA amplification (Supplementary Table S1).

Extraction of nuclei

Growing cells were trypsinized and washed twice with cold phosphate-buffered saline. Cells were resuspended in 1 ml of ice-cold RSB adding Nonidet P40 to a concentration of 1% and kept on ice for 10 min. After incubation, cells were centrifuged for 5 min at 800 *g* at 4 °C. The supernatant was discarded and nuclei were resuspended in RSB plus NP40. Samples were centrifuged for 5 min at 800 *g* at 4 °C. Nuclei were washed with RSB without NP40 and centrifuged for 5 min at 5 000 r.p.m. at 4 °C. The supernatant was discarded and the nuclei were resuspended in the corresponding buffer.

MspI accessibility assay

Nuclei were resuspended in 1x *MspI* buffer to give 10⁶ nuclei per 400 μl. Nuclei from each cell line were digested in a series of increasing *MspI* restriction enzyme (Roche Molecular Biochemicals, Indianapolis, IN, USA) concentrations (0, 100 and 400 U/ml) at 37 °C for 1 h. Reactions were stopped by adding 100 μl of stop solution (20 mM Tris-HCl pH 7.5, 0.6 M NaCl, 1% SDS, 10 mM EDTA and 400 μg/ml proteinase K) and incubating at 37 °C for 2 h. DNA was purified by phenol/chloroform extraction and ethanol precipitation. Amplicons were amplified and quantified through real-time PCR in an Applied Biosystems 7900HT Fast Real-Time PCR System. Results were normalized with respect to a region that does not have any *MspI* restriction site. The results shown are the means of at least three independent experiments amplifying each sample in triplicate. PCR primers are shown in Supplementary Table S1.

In vitro methylation footprinting

We adapted the methyltransferase-based single-promoter analysis assay protocol²¹ for use with methylated sequences. We substituted *SssI* methyltransferase for *MspI*, *HaeIII* and *AluI* methyltransferases (New England Biolabs, Ipswich, MA, USA). Extracted nuclei (~10⁶) were incubated for 30 min first with 60 U of *HaeIII*, then with 60 U of *MspI* and finally with 60 U of *AluI* methyltransferases. A 1x phosphate-buffered saline wash was done between incubations and nuclei were resuspended in the corresponding buffer. The final reaction was stopped by adding 100 μl of stop solution (20 mM Tris-HCl pH 7.5, 0.6 M NaCl, 1% SDS, 10 mM EDTA and 400 μg/ml proteinase K) and incubating at 37 °C for 2 h. DNA was purified by phenol/chloroform extraction and ethanol precipitation. Naked DNA was used as a positive control to check the efficiency of the methyltransferases.

Obtaining nucleosomal DNA

To prepare mononucleosomal DNA, 10⁶ nuclei were resuspended in 500 μl MNase buffer. Then, 500 U/ml of MNase (Roche) were added and tubes

were incubated for 0.5–10 min at 37 °C. The reaction was stopped by adding EDTA to a final concentration of 20 mM and SDS to a final concentration of 1%. The suspension was centrifuged at 14 000 r.p.m. for 15 min. The supernatant containing the nuclease digested nuclei was incubated with 0.1 mg/ml proteinase K overnight at 37 °C. DNA was treated with RNase, extracted with phenol/chloroform, precipitated with ethanol and finally resuspended in TE buffer. The DNA obtained was run on an agarose gel to produce a nucleosomal DNA ladder. The mononucleosomal band, corresponding to a 147 bp band, was recovered from the gel and the DNA was purified.

DNA methylation and nucleosome positioning profiling using bead arrays

Methylation was assessed at 1505 CpG sites using Illumina Goldengate Methylation Arrays, as previously described. In this work, genomic DNA from HCT-116 and DKO cell lines was hybridized, wherein all the sequences with a difference of at least 70% between the two cell lines were considered to be hypermethylated in HCT-116 (genomic HCT116 hybridization signal–genomic DKO hybridization signal ≥ 0.7). We next determined which of the methylated sequences were protected from MNase digestion due to nucleosome occupancy. The hybridization results of HCT116 mononucleosomal DNA were compared with DKO genomic DNA hybridization results, the sequences with an enrichment of 70% in the hybridization signal being considered to be protected (mononucleosomal HCT-116 hybridization signal–genomic DKO hybridization signal ≥ 0.7).

Growth assays

Doubling time determination, colony formation, MTT and nude mice subcutaneous growth assays are explained in detail in Supplementary Methods.

CONFLICT OF INTEREST

The authors declare no conflict of interest.

ACKNOWLEDGEMENTS

This work was supported by the Ministerio de Ciencia e Innovación (MICINN), grant number SAF2011–22803 (ME), the European Research Council (ERC) Advanced Grant EPINORC (ME), Cellex Foundation, the Health and Science Departments of the Catalan Government (Generalitat de Catalunya) and a Fondo de Investigaciones Sanitarias Grant PI08–1345 (ME). AP is a Sara Borrell Postdoctoral Fellow. ME is an ICREA Research Professor.

REFERENCES

- Esteller M. Cancer epigenomics: DNA methylomes and histone-modification maps. *Nat Rev Genet* 2007; **8**: 286–298.
- Shen L, Kondo Y, Guo Y, Zhang J, Zhang L, Ahmed S et al. Genome-wide profiling of DNA methylation reveals a class of normally methylated CpG island promoters. *PLoS Genet* 2007; **3**: 2023–2036.
- Portela A, Esteller M. Epigenetic modifications and human disease. *Nat Biotechnol* 2010; **28**: 1057–1068.
- Li B, Carey M, Workman JL. The role of chromatin during transcription. *Cell* 2007; **128**: 707–719.
- Hodges C, Bintu L, Lubkowska L, Kashlev M, Bustamante C. Nucleosomal fluctuations govern the transcription dynamics of RNA polymerase II. *Science* 2009; **325**: 626–628.
- Jiang C, Pugh BF. Nucleosome positioning and gene regulation: advances through genomics. *Nat Rev Genet* 2009; **10**: 161–172.
- Schones DE, Cui K, Cuddapah S, Roh TY, Barski A, Wang Z et al. Dynamic regulation of nucleosome positioning in the human genome. *Cell* 2008; **132**: 887–898.
- Cairns BR. The logic of chromatin architecture and remodelling at promoters. *Nature* 2009; **461**: 193–198.
- Lin JC, Jeong S, Liang G, Takai D, Fatemi M, Tsai YC et al. Role of nucleosomal occupancy in the epigenetic silencing of the MLH1 CpG island. *Cancer Cell* 2007; **12**: 432–444.
- Han H, Cortez CC, Yang X, Nichols PW, Jones PA, Liang GDNA. Methylation directly silences genes with non-CpG island promoters and establishes a nucleosome occupied promoter. *Hum Mol Genet* 2011; **20**: 4299–4310.
- Chodavarapu RK, Feng S, Bernatavichute YV, Chen PY, Stroud H, Yu Y et al. Relationship between nucleosome positioning and DNA methylation. *Nature* 2010; **466**: 388–392.
- Felle M, Hoffmeister H, Rothhammer J, Fuchs A, Exler JH, Langst G. Nucleosomes protect DNA from DNA methylation *in vivo* and *in vitro*. *Nucleic Acids Res* 2012; **39**: 6956–6969.
- Bartke T, Vermeulen M, Khemalce B, Robson SC, Mann M, Kouzarides T. Nucleosome-interacting proteins regulated by DNA and histone methylation. *Cell* 2010; **143**: 470–484.
- Lee JY, Lee TH. Effects of DNA methylation on the structure of nucleosomes. *J Am Chem Soc* 2011; **134**: 173–175.
- Rhee I, Bachman KE, Park BH, Jair KW, Yen RW, Schuebel KE et al. DNMT1 and DNMT3b cooperate to silence genes in human cancer cells. *Nature* 2002; **416**: 552–556.
- Jacinto FV, Ballestar E, Ropero S, Esteller M. Discovery of epigenetically silenced genes by methylated DNA immunoprecipitation in colon cancer cells. *Cancer Res* 2007; **67**: 11481–11486.
- Schuebel KE, Chen W, Cope L, Glockner SC, Suzuki H, Yi JM et al. Comparing the DNA hypermethylome with gene mutations in human colorectal cancer. *PLoS Genet* 2007; **3**: 1709–1723.
- De Carvalho DD, Sharma S, You JS, Su SF, Taberlay PC, Kelly TK et al. DNA methylation screening identifies driver epigenetic events of cancer cell survival. *Cancer Cell* 2012; **21**: 655–667.
- Youssef EM, Estecio MR, Issa JP. Methylation and regulation of expression of different retinoic acid receptor beta isoforms in human colon cancer. *Cancer Biol Ther* 2004; **3**: 82–86.
- Sandoval J, Heyn H, Moran S, Serra-Musach J, Pujana MA, Bibikova M et al. Validation of a DNA methylation microarray for 450,000 CpG sites in the human genome. *Epigenetics* 2011; **6**: 692–702.
- Fatemi M, Pao MM, Jeong S, Gal-Yam EN, Egger G, Weisenberger DJ et al. Footprinting of mammalian promoters: use of a CpG DNA methyltransferase revealing nucleosome positions at a single molecule level. *Nucleic Acids Res* 2005; **33**: e176.
- Bibikova M, Lin Z, Zhou L, Chudin E, Garcia EW, Wu B et al. High-throughput DNA methylation profiling using universal bead arrays. *Genome Res* 2006; **16**: 383–393.
- Byun HM, Siegmund KD, Pan F, Weisenberger DJ, Kanel G, Laird PW et al. Epigenetic profiling of somatic tissues from human autopsy specimens identifies tissue- and individual-specific DNA methylation patterns. *Hum Mol Genet* 2009; **18**: 4808–4817.
- Christensen BC, Marsit CJ, Houseman EA, Godleski JJ, Longacker JL, Zheng S et al. Differentiation of lung adenocarcinoma, pleural mesothelioma, and nonmalignant pulmonary tissues using DNA methylation profiles. *Cancer Res* 2009; **69**: 6315–6321.
- Fernandez AF, Assenov Y, Martin-Subero JI, Balint B, Siebert R, Taniguchi H et al. A DNA methylation fingerprint of 1628 human samples. *Genome Res* 2012; **22**: 407–419.
- Carmona FJ, Villanueva A, Vidal A, Munoz C, Puertas S, Penin RM et al. Epigenetic disruption of cadherin-11 in human cancer metastasis. *J Pathol* 2011; **228**: 230–240.
- Gowher H, Stockdale CJ, Goyal R, Ferreira H, Owen-Hughes T, Jeltsch A. *De novo* methylation of nucleosomal DNA by the mammalian Dnmt1 and Dnmt3A DNA methyltransferases. *Biochemistry* 2005; **44**: 9899–9904.
- Shen L, Gao G, Zhang Y, Zhang H, Ye Z, Huang S et al. A single amino acid substitution confers enhanced methylation activity of mammalian Dnmt3b on chromatin DNA. *Nucleic Acids Res* 2010; **38**: 6054–6064.
- Jeong S, Liang G, Sharma S, Lin JC, Choi SH, Han H et al. Selective anchoring of DNA methyltransferases 3A and 3B to nucleosomes containing methylated DNA. *Mol Cell Biol* 2009; **29**: 5366–5376.
- Sharma S, De Carvalho DD, Jeong S, Jones PA, Liang G. Nucleosomes containing methylated dna stabilize dna methyltransferases 3A/3B and ensure faithful epigenetic inheritance. *PLoS Genet* 2011; **7**: e1001286.
- Pandiyani K, You JS, Yang X, Dai C, Zhou XJ, Baylin SB et al. Functional DNA demethylation is accompanied by chromatin accessibility. *Nucleic Acids Res* 2013; **41**: 3973–3985.
- Davey CS, Pennings S, Reilly C, Meehan RR, Allan J. A determining influence for CpG dinucleotides on nucleosome positioning *in vitro*. *Nucleic Acids Res* 2004; **32**: 4322–4331.
- Pennings S, Allan J, Davey CS. DNA methylation, nucleosome formation and positioning. *Brief Funct Genomic Proteomic* 2005; **3**: 351–361.
- Kelly TK, Liu Y, Lay FD, Liang G, Berman BP, Jones PA. Genome-wide mapping of nucleosome positioning and DNA methylation within individual DNA molecules. *Genome Res* 2012; **22**: 2497–2506.



This work is licensed under a Creative Commons Attribution-NonCommercial-NoDerivs 3.0 Unported License. To view a copy of this license, visit <http://creativecommons.org/licenses/by-nc-nd/3.0/>

Supplementary Information accompanies this paper on the Oncogene website (<http://www.nature.com/onc>)